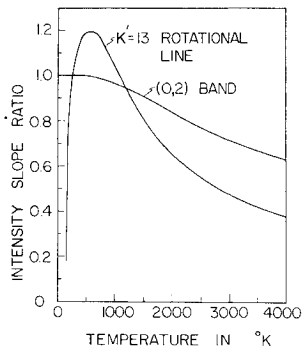

Fig. 2 Typical intensity slope ratios: $S(T_V)/S(T_c)$ and $R(T_R)/R(T_c)$.

(room temperature). Typical values of the slope ratios $S(T_V)/S(T_c)$ and $R(T_R)/R(T_c)$ are shown in Fig. 2.

To determine the nitrogen number density from the measurement of a line intensity, a room temperature calibration must be performed to determine the factor $C_1S(T_c)\ R(T_c)$. The constant C_1 can be considered to include the sensitivity of the measuring system. The N_2 number density is determined with the measured line intensity and the calibration curve, with the slope of the calibration curve modified by the slope ratios $S(T_V)/S(T_c)$ and $R(T_R)/R(T_c)$. Both the rotational and vibrational temperatures must be measured to determine the slope ratios. Note that serious errors in density measurement result if the effects of rotational and vibrational temperature differences between test and calibration conditions are ignored.

The N_2 number density also can be determined by measuring the intensity of a particular band. The intensity of a given band is[2]

$$I_{v',v''} = [S(T_V)/S(T_c)][C_2S(T_c)]N_{N_2} \qquad (9)$$

where $S(T_V)$ is given by Eq. (6). As with the line intensity method, a room temperature calibration of the band intensity must be performed to determine the slope $C_2S(T_c)$, and the vibrational temperature in the gas must be measured so that the slope ratio $S(T_V)/S(T_c)$ can be obtained. In this case, the rotational temperature need not be measured along with the band intensity to obtain valid density results. However, for vibrational temperatures in excess of 1000°K, the effect of vibrational excitation on the band intensity cannot be ignored.

Finally, under certain circumstances, the number density can be determined by measuring the total intensity of the radiation emitted by the electron beam. However, there are difficulties associated with a total intensity measurement which do not exist with the other methods discussed. In addition to the radiation of the N_2^+ system, bands from the second positive system of N_2 also appear in the spectrum.[2] Although the N_2^+ radiation intensity could be corrected for a varying vibrational temperature, it is unclear how the intensity of the N_2 system relative to that of the N_2^+ system changes with changing vibrational temperature. Radiation from metastable electronic energy states also may be included in the total emissive intensity. The radiation from metastable states is responsible for the "afterglow" observed in flowing gases. Normally, calibration of the total intensity as a function of N_2 number density is performed with no gas flow and the calibration then is applied to determine the density in a flowing system. However, the radiation from metastable states included in the intensities of the static calibration would be swept downstream by the gas flow and out of range of the detector, introducing errors in the density measurement. For nitrogen or air excited by an electron beam, no significant radiation from metastable states has been observed. For other gases, the possible existence of afterglow should be examined before the total radiation intensity is employed for density measurement.

From these discussions it can be concluded that the measurement of number density with the intensity of a single rotational line requires a simultaneous measurement of both the rotational and vibrational temperatures. The measurement of a band intensity is most convenient when there is vibrational excitation in the test gas. For vibrational temperatures below approximately 1000°K, either a band intensity or the total radiation intensity can be employed.

The measurement of density with an electron beam is based entirely on the linearity of a line or band intensity with number density. Collision quenching of the excited ions occurs with increased frequency as the gas density is increased, eventually causing nonlinearity in the density-intensity calibration. It appears that density data can be obtained for pressures (room temperature) near 500-μ Hg. In any case, the influence of rotational and vibrational temperature differences between calibration and test conditions cannot be ignored to obtain valid density data.

References

[1] Muntz, E. P., "Measurement of rotational temperature, vibrational temperature, and molecule concentration in non-radiating flows of low density nitrogen," University of Toronto Institute of Aerophysics Rept. 71 (April 1961).

[2] Petrie, S. L., Pierce, G. A., and Fishburne, E. S., "Analysis of the thermo-chemical state of an expanded air plasma," Ohio State University Aerodynamic Lab., Air Force Flight Dynamics Lab. Rept. AFFDL-TR-64-191 (1965).

[3] Gadamer, E. O., "Measurement of the density distribution in a rarefied gas flow using the fluorescence induced by a thin electron beam," University of Toronto Institute of Aerophysics Rept. 83 (March 1962).

[4] MacArthur, R. C., Stevenson, L. M., and Budell, J., "Flow visualization and quantitative gas density measurements in rarefied gas flows," Cornell Aeronautical Lab., Inc., Aeronautical Systems Division Tech. Doc. Rept. ASD-TDR-62-793 (December 1962).

[5] Sebacher, D. I. and Duckett, R. J., "A spectrographic analysis of a 1-foot hypersonic arc tunnel airstream using an electron beam probe," NASA Langley Research Center TR R-214 (December 1964).

[6] Petrie, S. L., "Flow field analyses in a low density arc-heated wind tunnel," *Proceedings of the 1965 Heat Transfer and Fluid Mechanics Institute*, edited by A. F. Charwat et al. (Stanford University Press, Stanford, Calif., 1965).

[7] Muntz, E. P. and Marsden, D. J., "Electron excitation applied to the experimental investigation of rarefied gas flows," *Rarefied Gas Dynamics*, edited by J. E. Laurmann (Academic Press Inc., New York, 1963), Vol. II.

Eccentric Discontinuities in Unsymmetrically Loaded Shells of Revolution

RALPH M. VERETTE*
North American Aviation Inc., Downey, Calif.

AND

R. B. MATTHIESEN†
University of California at Los Angeles, Los Angeles, Calif.

Introduction

A QUESTION that arises in the analysis of discontinuities in shells is the effect of eccentricities in the middle surface on the magnitude of the discontinuity stresses. In the

Received October 13, 1965; revision received May 12, 1966.

* Senior Research Engineer, Structural Sciences Department, Space and Information Systems Division.

† Assistant Professor of Engineering.

Table 1 Dimensions and physical properties of cylinders used in numerical example

Configuration	t^- in.	t^+ in.	R^- in.	R^+ in.	L^- in.	L^+ in.	μ in.	E^- psi	E^+ psi	ν^-	ν^+
Continuous inner surface	0.082	0.205	2.831	2.8925	6.00	6.50	0.123	10^7	10^7	0.3	0.3
Continuous middle surface	0.082	0.205	2.8925	2.8925	6.00	6.50	0.0615	10^7	10^7	0.3	0.3
Continuous outer surface	0.082	0.205	2.954	2.8925	6.00	6.50	0.00	10^7	10^7	0.3	0.3

case of symmetric loads, the effect is held to be small. This note summarizes a study of this effect when the loading is unsymmetric.

Analysis

Shells of revolution which possess eccentric discontinuities in the reference surface along the meridian may be analyzed conveniently by a slight generalization of the material presented in Ref. 1. A typical discontinuity location and the associated finite difference stations are shown in Fig. 1. Note that, in the present formulation, the discontinuity occurs midway between $j-1$ and j^- on the portion of the shell behind the discontinuity, and midway between $j+1$ and j^+ on the portion of the shell ahead of the discontinuity.

In a manner similar to that given in Ref. 1, the conditions of geometric compatibility at the discontinuity station can be given by:

$$
\begin{aligned}
(u_\xi)_{j+1/2} &= [(u_\xi)_{j-1/2} + (\phi_\xi)_{j-1/2}E_{cc}]\cos\psi - w_{j-1/2}\sin\psi \\
(u_\theta)_{j+1/2} &= (u_\theta)_{j-1/2} + E_{cc}(\phi_\theta)_{j-1/2} \\
w_{j+1/2} &= [(u_\xi)_{j-1/2} + E_{cc}(\phi_\xi)_{j-1/2}]\sin\psi + w_{j-1/2}\cos\psi \\
(\phi_\xi)_{j+1/2} &= (\phi_\xi)_{j-1/2}
\end{aligned}
$$

and equilibrium requires that

$$
\begin{aligned}
(t_\xi)_{j+1/2} &= (t_\xi)_{j-1/2}\cos\psi - (\hat{f}_\xi)_{j-1/2}\sin\psi \\
(\hat{t}_{\xi\theta})_{j+1/2} &= (\hat{t}_{\xi\theta})_{j-1/2} \\
(\hat{f}_\xi)_{j+1/2} &= (t_\xi)_{j-1/2}\sin\psi + (\hat{f}_\xi)_{j-1/2}\cos\psi \\
(m_\xi)_{j+1/2} &= (m_\xi)_{j-1/2} - E_{cc}(t_\xi)_{j-1/2}
\end{aligned}
$$

Using Eq. 57 of Ref. 1, the previous two sets of equations can be summarized in matrix form as:

$$
\begin{aligned}
y_{j+1/2} &= \Psi y_{j-1/2} \\
z_{j+1/2} &= \Phi z_{j-1/2} + \Upsilon y_{j-1/2}
\end{aligned}
\tag{1}
$$

where

$$
\Phi = \Psi + E_{cc}\begin{bmatrix} 0 & 0 & 0 & 0 \\ 0 & \omega_{\theta_{j-1/2}} & \dfrac{n}{\rho_{j-1/2}} & 0 \\ 0 & 0 & 0 & 0 \\ 0 & 0 & 0 & 0 \end{bmatrix}
$$

$$
\Upsilon = E_{cc}\begin{bmatrix} 0 & 0 & 0 & \cos\psi \\ 0 & 0 & 0 & 0 \\ 0 & 0 & 0 & \sin\psi \\ -1 & 0 & 0 & 0 \end{bmatrix}
$$

and E_{cc} = dimensionless eccentricity of reference surfaces measured along the radius of curvature behind the discontinuity point. (E_{cc} is positive outward.)

In equation form:

$$
E_{cc} = \frac{1}{a}\left[\mu + \frac{t^-}{2} - \frac{t^+}{2\cos\psi}\right]
$$

where μ = eccentricity of outer surface measured along the radius of curvature behind the discontinuity point. (μ is positive outward, hence the μ in Fig. 1 is a negative quantity.)‡

Utilizing Eq. (50), Ref. 1, and the second of Eqs. (1), an expression for $z_j{}^+$ is obtained as:

$$
z_j{}^+ = [\Phi + 2\Upsilon(H_{j-1/2}/\Delta^-) + \Upsilon J_{j-1/2}]z_j{}^- + 2\Upsilon f_{j-1/2} + [\Phi - 2\Upsilon(H_{j-1/2}/\Delta^-) + \Upsilon J_{j-1/2}]z_{j-1} - z_{j+1} \tag{2}
$$

Now the first of Eqs. (1) provides, along with Eq. (50), Ref. 1,

$$
\left(\frac{H_{j+1/2}}{\Delta^+} + \frac{J_{j+1/2}}{2}\right)z_{j+1} + \left(\frac{J_{j+1/2}}{2} - \frac{H_{j+1/2}}{\Delta^+}\right)z_j{}^+ - \Psi\left(\frac{H_{j-1/2}}{\Delta^-} + \frac{J_{j-1/2}}{2}\right)z_j{}^- - \Psi\left(\frac{J_{j-1/2}}{2} - \frac{H_{j-1/2}}{\Delta^-}\right)z_{j-1} = \Psi f_{j-1/2} - f_{j+1/2} \tag{3}
$$

Substituting Eq. (2) into Eq. (3), we obtain:

$$
\begin{aligned}
&\frac{2H_{j+1/2}}{\Delta^+}z_{j+1} + \left[-\Psi\left(\frac{H_{j-1/2}}{\Delta^-} + \frac{J_{j-1/2}}{2}\right) + \left(\frac{J_{j+1/2}}{2} - \frac{H_{j+1/2}}{\Delta^+}\right)\left(\Phi + 2\Upsilon\frac{H_{j-1/2}}{\Delta^-} + \Upsilon J_{j-1/2}\right)\right]z_j{}^- + \\
&\left[-\Psi\left(\frac{J_{j-1/2}}{2} - \frac{H_{j-1/2}}{\Delta^-}\right) + \left(\frac{J_{j+1/2}}{2} - \frac{H_{j+1/2}}{\Delta^+}\right)\times\left(\Phi - 2\Upsilon\frac{H_{j-1/2}}{\Delta^-} + \Upsilon J_{j-1/2}\right)\right]z_{j-1} = \Psi f_{j-1/2} - \\
&f_{j+1/2} + 2\frac{H_{j+1/2}}{\Delta^+}\Upsilon f_{j-1/2} - J_{j+1/2}\Upsilon f_{j-1/2}
\end{aligned}
\tag{4}
$$

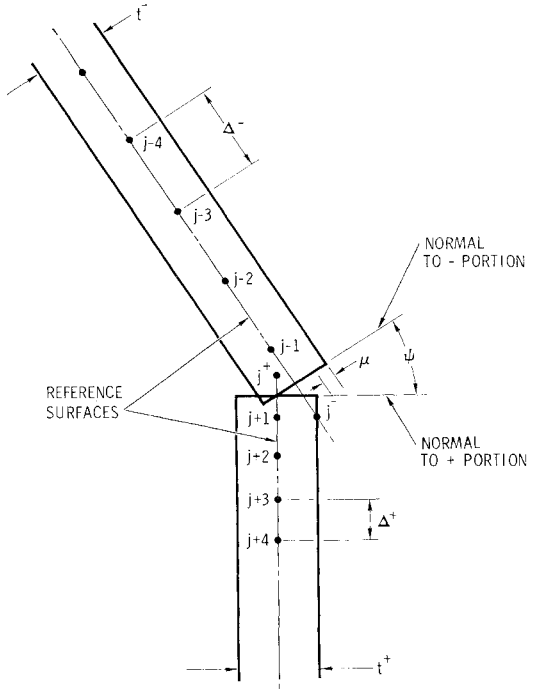

Fig. 1 Physical model for an eccentric discontinuity.

‡ All quantities appearing in Eq. (1) and all subsequent equations, unless explicitly defined in this paper, retain their definitions from Ref. 1.

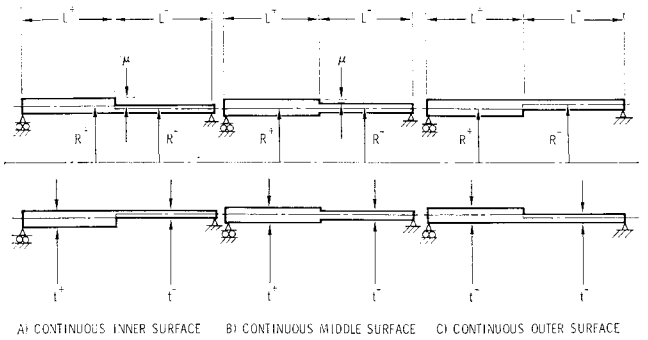

Fig. 2 Cylinders with discontinuities.

For the point $i = j^-$, the A_i, B_i, C_i, and g_i matrices of Eq. (66), Ref. 1, are defined by Eq. (4). At $i = j + 1$, Eq. (39),[1] and Eq. (2) yield:

$$\left(\frac{2E_i}{\Delta^+} + F_i\right) z_{j+2} + \left(2\Delta^+ G_i - \frac{6E_i}{\Delta^+} + F_i\right) z_{j+1} + \left(\frac{2E_i}{\Delta^+} - F_i\right)\left(\Phi + 2\Upsilon \frac{H_{j-1/2}}{\Delta^-} + \Upsilon J_{j-1/2}\right) z_j^- + \left(\frac{2E_i}{\Delta^+} - F_i\right)\left(\Phi - 2\Upsilon \frac{H_{j-1/2}}{\Delta^-} + \Upsilon J_{j-1/2}\right) z_{j-1} = 2\Delta^+ e_i - \left(\frac{2E_i}{\Delta^+} - F_i\right) 2\Upsilon f_{j-1/2} \quad (5)$$

Thus, at stations just past the discontinuity (i.e., at $i = i + 1$), Eq. (66),[1] should be generalized to:

$$A_i z_{i+1} + B_i z_i + C_i z_{i-1} + D_i z_{i-2} = g_i \quad (6)$$

where the A_i, B_i, C_i, D_i, and g_i matrices are defined by Eq. (5).

Having the A_i, B_i, C_i, D_i, and g_i matrices at all stations, the solution proceeds as in Ref. 1. However, at $i = j + 1$, in place of Eqs. (74),[1] we have:

$$P_i = [B_i - C_i P_{i-1} + D_i P_{i-2} P_{i-1}]^{-1} A_i$$
$$x_i = [B_i - C_i P_{i-1} + D_i P_{i-2} P_{i-1}]^{-1} \times [g_i - D_i x_{i-2} - (C_i - D_i P_{i-2}) x_{i-1}] \quad (7)$$

Also, since j^- and j^+ both are associated with $i = j$, we set $P_j^- = P_j^+$ and $x_j^- = x_j^+$. Note that this procedure temporarily will give an incorrect result for z_j^+, giving it the value rightfully associated with $i = j^-$. The neighboring points all receive their correct z values. Having completed the z calculation procedure, the correct value of z^+ is obtained easily using Eq. (2).

Numerical Example

As an example of the aforementioned procedure, consider the three cylinders, (Fig. 2) with the Table 1 dimensions and properties. The stress distributions in these cylinders were given in Ref. 2 for the case of an axisymmetric internal pressure of 621 psi. For this example, suppose the cylinders are subjected to an unsymmetrical uniform internal pressure of 621 cosθ psi. The resulting meridional stresses at $\theta = 0°$ in the inner and outer extreme fibers are shown in Figs. 3 and 4. Results indicate that, at any circumferential location, the type of discontinuity (i.e., a continuous inner surface, continuous reference surface, or continuous outer surface) has a pronounced effect on the resulting stress distributions when the cylinder is loaded unsymmetrically. Comparing these results with the curves of Ref. 2, we see that the stress increasing effect of eccentric discontinuities is much more important for the cosine loading than for axisymmetric loading in the case of meridional stresses. A similar conclusion has been reached for the case of circumferential stresses in Ref. 3 where, in addition, comparisons are made between the results

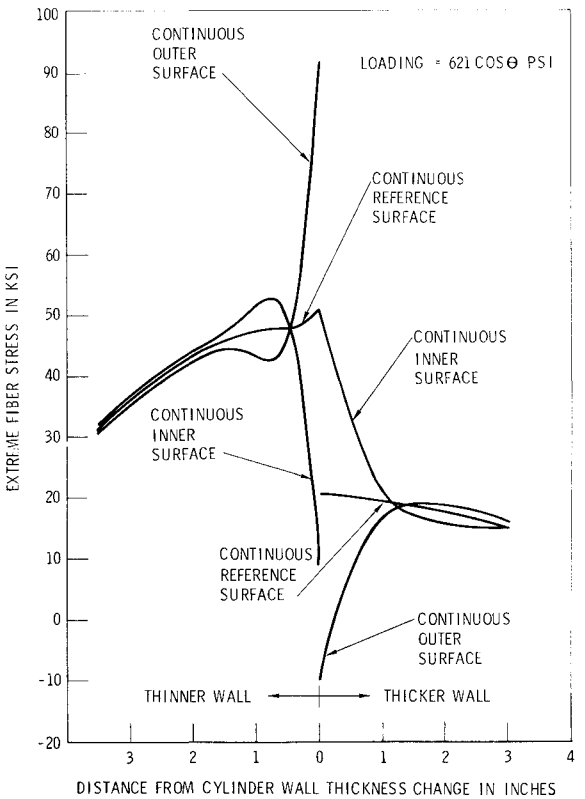

Fig. 3 Meridional stresses in inner extreme fibers at $\theta = 0°$.

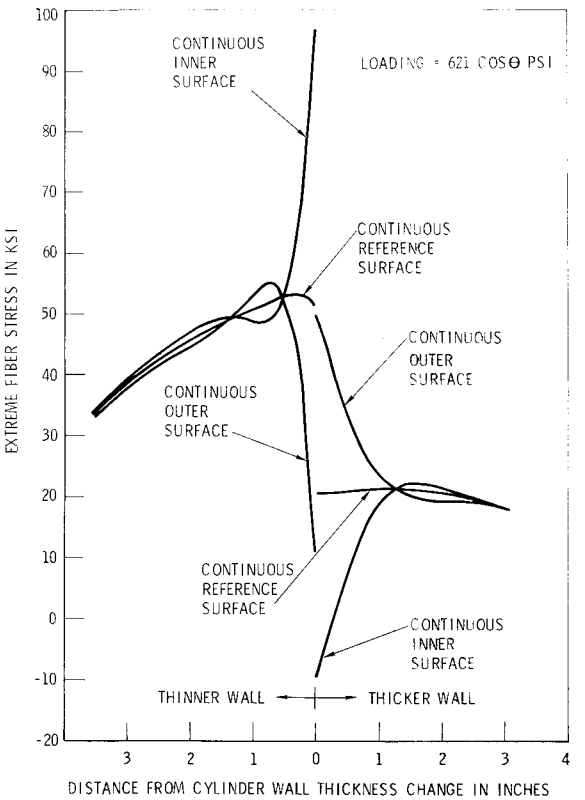

Fig. 4 Meridional stresses in outer extreme fibers at $\theta = 0°$.

of Ref. 2 and those of the previous procedure for axisymmetric loads.

References

[1] Budiansky, B. and Radkowski, P. P., "Numerical analysis of unsymmetrical bending of shells of revolution," AIAA J. 1, 1833–1842 (1963).

[2] Morgan, W. C. and Bizon, P. T., "Experimental investigation of stress distributions near abrupt change in wall thickness in thin-walled pressurized cylinders," NASA Lewis Research Center, Cleveland, Ohio, TN D-1200 (June 1962).

[3] Verette, R. M. and Matthiesen, R. B., "On the analysis of discontinuities in shells of revolution subjected to unsymmetrical loads," North American Aviation, Space and Information Systems Div., Structures NAAS & IDS TR-134 (Sept. 1965).

Terminal Guidance for Continuous Powered Space Vehicles

B. D. Tapley* and W. T. Fowler†
University of Texas, Austin, Texas

In the investigation presented here, a method for determining the guidance procedure for a continuous powered space vehicle very similar to that suggested in Ref. 1 is proposed. One advantage of the proposed method is that the arbitrary weighting matrix, which is a characteristic of the scheme discussed in Ref. 1, is replaced by a uniquely specified matrix. Furthermore, a state prediction scheme is given which is general enough to handle all terminal constraint requirements. The control procedure is developed by requiring that the change in the value of the original performance index be a minimum. That is, the control deviation program seeks to reoptimize the performance index associated with the nominal trajectory.

If $x(t)$ represents the deviation in the state and $u(t)$ represents the deviation in the control, then the state and control program associated with the actual trajectory can be specified as $X(t) = X^*(t) + x(t)$ and $U(t) = U^*(t) + u(t)$ where $X^*(t)$ and $U^*(t)$ represent a reference state history and control program. By expanding the nonlinear equations of motion in a Taylor's series about the reference trajectory at each point in time, the following expression for the state deviation histories can be obtained:

$$\dot{x} = Ax + Bu \tag{1}$$

where $A = (F_X)^*$ and $B = (F_U)^*$[2]. The symbol $(\ )^*$ indicates that the quantity in the parenthesis is evaluated on the reference trajectory.

Assume that the guidance maneuver is to be carried out in such a way that the change in the original (or nominal) performance index is minimized. If the reference trajectory is optimal, the increase in the value of the performance index associated with following some trajectory other than the optimal reference trajectory can be approximated by

$$\Delta P = \int_{t_0}^{t_f} E(X^*, \dot{X}^*, \dot{X}, t)dt$$

where E is the Weierstrass E-function (Ref. 3). For a Mayer formulation of the optimization problem, $E = H(X^*, U, t) - H(X^*, U^*, t)$. A necessary condition for a minimum value of the nominal performance index is $E \geq 0$. For a sufficiently small deviation in the nominal control program, E can be approximated by the following expression $E = (U - U^*)H^*_{UU}\cdot(U - U^*) = \frac{1}{2}u^T H_{UU}{}^* u$ where $H_{UU}{}^*$ is an $m \times m$ matrix. With this approximation, the expression for ΔP becomes

$$\Delta P = \int_{t_0}^{t_f} \tfrac{1}{2}(u^T H_{UU}{}^* u)dt \tag{2}$$

The problem to be considered can be stated now as follows: Determine the control deviation program $u(t)$ which will minimize ΔP subject to the differential equations $\dot{x} = Ax + Bu$ while satisfying the terminal conditions $M(x_f, t_f) = 0$. The solution to this problem requires that the following conditions be satisfied:

$$\dot{x} = Ax + Bu \qquad (x)_0 = x_0 \qquad \dot{\lambda}^T = -\lambda^T A$$
$$(\lambda^T - \nu^T M_x)_{tf} dx_f = 0 \qquad 0 = H_{UU}{}^* u + B^T \lambda$$
$$(\nu^T M_t + \lambda^T \dot{x})_{tf} dt_f = 0 \tag{3}$$

From the third of Eqs. (3), the optimum control deviation program is given as $u(t) = -(H_{UU}{}^*)^{-1}B^T\lambda(t)$. A complete solution requires only that the $\lambda(t)$ be determined. The $\lambda(t)$ are governed by the second of Eqs. (3). They can be expressed as $\lambda(t) = \Phi^T(t, t_f)\lambda(t_f)$ where $\Phi^T(t, t_f)$ is determined by integrating the second of Eqs. (3), backward from t_f, n times with the starting conditions $\lambda_{ij} = \delta_{ij}$, $(i, j, = 1 \ldots n)$ (δ_{ij} is the Kronecker δ). With these conditions, $\Phi(t_f, t_f) = I$, the identity matrix. If dx_f is not zero, then from the fourth of Eqs. (3), $\lambda^T(t_f) = \nu^T M_{x_f}$. Hence, $u(t)$ can be expressed as follows

$$u(t) = -(H_{UU}{}^*)^{-1}B^T\Phi(t, t_f)M_{x_f}{}^T\nu \tag{4}$$

Note that the constants ν are unspecified.

If the first of Eqs. (3) is premultiplied by λ^T and added to the second of Eqs. (3) postmultiplied by x, the resulting expression will yield

$$(\lambda^T x)_{t_f} = (\lambda^T x)_{t_0} + \int_{t_0}^{t_f} \lambda^T B\, u\, dt \tag{5}$$

The expressions for $\lambda^T(t)$ and $u(t)$ can be substituted into Eq. (5) to obtain the following expression:

$$\lambda_f{}^T x_f = \lambda_f{}^T[\Phi(t_0, t_f)x_0 - J(t_0, t_f)M_{x_f}{}^T \nu] \tag{6}$$

where

$$J(t, t_f) = \int_t^{t_f} [\Phi(\tau, t_f)B\, H_{UU}{}^{*-1}\, B^T\Phi^T(\tau, t_f)]d\tau$$

Equation (6) can be used to determine the constants ν and also as the starting point for developing the state prediction scheme.

Consider the fixed final time problem where t_f is specified to be the final time associated with the nominal trajectory. If the conditions

$$(\lambda_j{}^T)_{t_f} = (\partial M^j/\partial x_f) \qquad j = 1, \ldots p \tag{7}$$

are used in Eq. (6) the resulting set of p independent conditions can be expressed

$$M_{x_f}x_f = M_{x_f}[\Phi(t_0, t_f)x_0 - J(t_0, t_f)M_{x_f}{}^T\nu] \tag{8}$$

where $M_{x_f} = (\partial M/\partial x_f)$. Now, provided that $[M_{x_f}J(t_0, t_f)M_{x_f}{}^T]$ is nonsingular, Eq. (8) can be solved for the p unknown constants ν, i.e.,

$$\nu = -[M_{x_f}J(t_0, t_f)M_{x_f}{}^T]^{-1}M_{x_f}[x_f - \Phi(t_0, t_f)x_0] \tag{9}$$

The following form for the optimal control deviation program

Presented as Preprint 65-696 at the AIAA/ION Astrodynamics Specialist Conference, Monterey, Calif., September 16–17, 1965; submitted December 1, 1965; revision received May 19, 1966. This work was supported by NASA under Grant NsG-551.

* Associate Professor, Department of Aerospace Engineering and Engineering Mechanics. Member AIAA

† Assistant Professor, Department of Engineering Mechanics.